Electrostatic Contributions to Heat Capacity Changes of DNA-Ligand Binding

Kelly Gallagher and Kim Sharp

The Johnson Research Foundation, Department of Biochemistry and Biophysics, University of Pennsylvania, Philadelphia, Pennsylvania 19104-6059 USA

ABSTRACT   Significant heat capacity changes (ΔC_p) often accompany protein unfolding, protein binding, and specific DNA-ligand binding reactions. Such changes are widely used to analyze contributions arising from hydrophobic and polar hydration. Current models relate the magnitude of ΔC_p to the solvent accessible surface area (ASA) of the molecule. However, for many binding systems—particularly those involving non-peptide ligands—these models predict a ΔC_p that is significantly different from the experimentally measured value. Electrostatic interactions provide a potential source of heat capacity changes and do not scale with ASA. Using finite-difference Poisson-Boltzmann methods (FDPB), we have determined the contribution of electrostatics to the ΔC_p associated with binding for DNA binding reactions involving the ligands DAPI, netropsin, lexitropsin, and the λ repressor binding domain.

INTRODUCTION

In order to accurately calculate the free energy of DNA-protein and DNA-ligand binding reactions, a detailed understanding of the forces that stabilize these complexes is required. Of prime importance among these forces is the interaction of a molecule with its solvent. Binding-associated heat capacity changes (ΔC_p) are believed to arise primarily from the influence of the solvent (Privalov and Gill, 1988; Sturtevant, 1977), unlike enthalpy, entropy, and free energy, which have contributions from a variety of sources. Thus, ΔC_p may be used to provide information about solvation decoupled from other effects. In addition, heat capacity changes differ from enthalpy and entropy because they are able to distinguish between polar and nonpolar hydration. For example, both hydrophobic and polar hydration are associated with a decrease in entropy, yet the ΔC_p values for these processes have opposite signs (Ben-Naim and Marcus, 1984; Murphy and Gill, 1990; Privalov and Makhatadze, 1993a, b).

Despite the potential for hydration heat capacity to provide a key to understanding solute-solvent interactions, there is as yet no good mechanistic model for ΔC_p that can be applied to macromolecular systems. This is due in part to the complex nature of ΔC_p as well as the limitations of existing computational techniques. The most detailed understanding of the relationship between hydration and heat capacity changes comes from the random network-explicit water model (Madan and Sharp, 1996, 1997; Sharp and Madan, 1997). This model has been used for the study of hydration heat capacities of a variety of small polar and nonpolar solutes, but it has not been applied to macromolecular binding. Currently, the only models applied to changes in heat capacity for binding reactions involving protein and DNA are based on changes in solvent accessible surface area (ASA). Area-based models employ empirical formulas that have been parametrized from protein folding and solute transfer data (Freire, 1995; Makhatadze and Privalov, 1990a, b; Murphy and Freire, 1992; Spolar et al., 1992). Thus, the hydrophobic effect provides the dominant term. These models only take into account short-range effects. Unfortunately, there is often a significant discrepancy between the experimental and ASA-calculated values of ΔC_p (Connelly et al., 1993). In the case of DNA-ligand binding this could be due to coupled folding and binding (Spolar and Record, 1994). Alternatively, hydration heat capacity parameters which have been derived from proteins may not be applicable to DNA hydration heat capacity. A recent detailed analysis of protein unfolding (Robertson and Murphy, 1997) illustrates another difficulty: the heat capacity data may be fit equally well with a number of different area-based models. Before these issues with area-based models can be resolved, however, it is necessary to establish whether there are contributions to heat capacity that would not scale with surface area and to determine the magnitude of any such contributions.

Our goal is to evaluate one contribution to ΔC_p that would not scale with surface area: long-range electrostatic interactions. Long-range electrostatic interactions are known to exert a strong influence on the enthalpies, entropies, and free energies of binding, and therefore might also affect their temperature dependence (i.e., ΔC_p). The most basic continuum representation of the solvent, the Born model, qualitatively reproduces the negative heat capacity change associated with ionic solvation (Madan and Sharp, 1996; Marcus, 1994). This observation implies that a continuum model of the solvent might be useful for deciphering the contribution of electrostatics to ΔC_p in more complicated charged molecules such as proteins and DNA. Finite difference (FD) methods for solving the nonlinear Poisson-

---

Boltzmann (PB) equation allow detailed information about a solute's complex shape and charge distribution, dielectric constant, and the ionic strength of the solvent to be considered within a continuum electrostatics framework. This technique has been successfully used for computing the electrostatic contribution to the free energy of binding (ΔG_{bind}^{el}) in protein-DNA and drug-DNA complexes (Hecht and Honig, 1995; Misra et al., 1994a, b; Zacharias et al., 1992, 1994) and has been extended to the calculation of the salt dependence of the free energy, entropy, and enthalpy (Sharp, 1995; Sharp et al., 1995).

In this work, we show how the FDPB method employing the nonlinear Poisson-Boltzmann equation can be extended to determine the electrostatic contribution to the heat capacity change, ΔC_p^{el}, for binding. The method is applied to the binding of the drugs DAPI, lexitropsin, and netropsin to the minor groove of DNA and the interaction of λ repressor binding domain (bd) with its operator. These systems were selected for several reasons. First, the drugs studied have no conformational change associated with binding. Moreover, electrostatics play a significant role in the binding of these positively charged ligands to the negatively charged DNA. Finally, high-resolution crystal structures are available for all of the complexes considered.

In addition to calculating the total electrostatic contribution to the heat capacity change, we show that there are three contributions to ΔC_p^{el}. The first comes from the rearrangement of water dipoles upon DNA-ligand binding (ΔC_p^{water}); the second, ΔC_p^{ions}, arises from the redistribution of mobile ions in the solvent upon binding; a third term, ΔC_p^{couple}, comes from the coupling between the dipolar and ionic terms. The highly charged nature of DNA results in the strong attraction of positively charged salt ions (counterions) and the repulsion of the corresponding co-ions. The ion atmosphere surrounding nucleic acids imparts a strong salt dependence to reactions in which the counterion distribution would change (e.g., the binding of a positively charged ligand), making it common practice to examine the salt dependence of binding to DNA (Anderson and Record, 1982, 1993; Record et al., 1990). Thus, we have also computed the salt dependence of ΔC_p^{el}, ΔC_p^{water}, and ΔC_p^{ions} for λ repressor binding domain-operator binding.

THEORY AND METHODS

Calculation of electrostatic potentials

The electrostatic potential distribution was calculated using the nonlinear Poisson-Boltzmann equation, which for a 1-1 salt is

$$\nabla \cdot \varepsilon(r)\nabla\phi(r) - 4\pi ec \sinh\left[\frac{e\phi(r)}{kT}\right] = -4\pi e\rho(r) \quad (1)$$

where $\phi(r)$ is the potential, e is the unit proton charge, k is the Boltzmann constant, T is the absolute temperature, $\varepsilon(r)$ and $\rho(r)$ are the dielectric constant and charge distributions, respectively, and c is the concentration of salt. The electrostatic free energy can then be determined from the calculated potential distribution by (Sharp and Honig, 1990):

$$\Delta G^{el} = \int\left[\frac{\rho^f\phi^f}{2} + \rho^f\phi^m + \frac{\rho^m\phi^m}{2} - (T\Delta S^m)\right]dV - \sum \Delta\Pi_i \quad (2)$$

where the superscripts f and m refer to contributions from the fixed and mobile charges, respectively, and the integration is over the solution volume (V). $\Delta\Pi_i$ is the net excess (or deficit) of ions of type i. $\int(\rho^f\phi^f/2)dV$ corresponds to the free energy required to charge the molecule in the absence of salt (i.e., in pure aqueous solution). The second term, $\int\rho^f\phi^m dV$, is the electrostatic free energy of interaction between the charged molecule and the equilibrium ion atmosphere. This is followed by $\int(\rho^m\phi^m/2)dV$, or the electrostatic self-energy of charging the ion atmosphere in the absence of the molecule. $\int T\Delta SdV + \sum\Delta\Pi_i$ is the organizational entropy associated with arranging the ions in the atmosphere.

The electrostatic component of the free energy change upon binding (ΔG_{bind}^{el}) was calculated for each ligand-DNA system according to

$$\Delta G_{bind}^{el} = \Delta G_{complex}^{el} - \Delta G_{DNA}^{el} - \Delta G_{ligand}^{el} \quad (3)$$

Electrostatic energies were calculated using the finite difference solution to the nonlinear Poisson-Boltzmann equation implemented in the program DelPhi (Gilson et al., 1988; Jayaram et al., 1989; Misra et al., 1994a, b; Nicholls and Honig, 1991; Sharp et al., 1990). Dielectric smoothing, charge anti-aliasing, and translational averaging techniques were employed to minimize the grid position dependence and increase the precision of the FDPB calculations (Bruccoleri et al., 1996). All calculations were done at an ionic strength of 0.10, with the exception of the λ repressor complex, for which the calculations were performed for a range of ionic strengths from 0 to 0.250 M.

Calculation of heat capacities

The heat capacity in the FDPB model can be obtained numerically by taking the second derivative of the electrostatic free energy with respect to temperature:

$$C_p = -T\left(\frac{\partial^2 G}{\partial T^2}\right)_P \quad (4)$$

Hence, the electrostatic contribution to the binding free energy, $\Delta\Delta G_{bind}^{el}$, was recomputed at 10° increments over the temperature range 273–373 K. ΔC_p^{el} was then determined by means of a linear least squares fit of the free energy data to the integrated van't Hoff equation:

$$k \ln K = k \ln K_0 + (\Delta H_0 - \Delta C_p T_0)\left(\frac{1}{T_0} - \frac{1}{T}\right) + \Delta C_p\ln\left(\frac{T}{T_0}\right) \quad (5)$$

where T_0 is the reference temperature, K_0 is the equilibrium constant at T_0, and ΔH_0 is the van't Hoff enthalpy at T_0. The fits were performed using the singular value decomposition (SVD) routine as described in Numerical Recipes (Press et al., 1986).

Examination of the Poisson-Boltzmann equation (Eq. 1) shows that the temperature dependence of the free energy comes from the explicit temperature dependence of the Boltzmann factor governing the distribution of mobile ions (the second term), and from an implicit dependence via the temperature dependence of the dielectric constant (the first term). Since the dielectric response of water involves a large, entropically unfavorable reorientation of water dipoles, it has a strong temperature dependence. This temperature dependence was incorporated into the calculations by using the appropriate experimentally determined value for the water dielectric constant ($\varepsilon_{solvent}$) at each temperature point (Lide, 1990). A dielectric constant of 4 was assigned to both DNA and ligands. Because the solute dielectric is much lower than the solvent dielectric and, from theoretical

grounds, will be much less sensitive to temperature (Gilson and Honig, 1986), the contribution of the solute dielectric to the heat capacity is expected to be much smaller than that of the solvent. Consequently, the temperature dependence of the solute dielectric was omitted in these calculations.

The complete second derivative of the free energy with respect to temperature (Eq. 4) is given by a sum of terms involving the partial derivatives with respect to the explicit (Boltzmann factor) and implicit (dielectric) dependence on temperature:

$$-T\frac{\partial^2 \Delta G}{\partial T^2} = -T\frac{\partial}{\partial T}\left(\frac{\partial \Delta G}{\partial T}\bigg|_{\varepsilon} + \frac{\partial \Delta G}{\partial \varepsilon}\bigg|_{B_f}\frac{\partial \varepsilon}{\partial T}\right)$$

$$= -T\frac{\partial}{\partial T}\left(\frac{\partial \Delta G}{\partial T}\bigg|_{\varepsilon} + \frac{\partial \Delta G}{\partial \varepsilon}\bigg|_{B_f}\frac{\partial \varepsilon}{\partial T}\right)_{\varepsilon} \quad (6)$$

$$-T\frac{\partial}{\partial T}\left(\frac{\partial \Delta G}{\partial T}\bigg|_{\varepsilon} + \frac{\partial \Delta G}{\partial \varepsilon}\bigg|_{B_f}\frac{\partial \varepsilon}{\partial T}\right)_{B_f}$$

where the subscript B_f denotes partial differentiation with a fixed Boltzmann factor. This leads to

$$\Delta C_p = \frac{\partial^2 \Delta G}{\partial T^2}\bigg|_{\varepsilon} + \frac{\partial^2 \Delta G}{\partial \varepsilon^2}\bigg|_{B_f}\left(\frac{\partial \varepsilon}{\partial T}\right)^2 + \text{cross-terms} \quad (7)$$

The cross-terms involve mixed derivatives of the type $(\partial^2 \Delta G/\partial T \partial \varepsilon)(\partial \varepsilon/\partial T)$ containing the differentials with respect to both Boltzmann factor and dielectric terms. In Eq. 7 the first term on the right-hand side provides the heat capacity change associated with the rearrangement of solvent ions (ΔC_p^{ions}), while the second term provides the heat capacity change associated with water dipole reorientation (ΔC_p^{water}), and the cross-terms provide the coupling between these two contributions. To compute these terms separately, two additional sets of calculations of ΔG_{bind}^{el} as a function of T were performed: 1) holding $\varepsilon_{solvent}$ constant at all temperatures, providing ΔC_p^{ions}, and 2) using a temperature-dependent $\varepsilon_{solvent}$ while keeping the temperature constant in the ionic strength term of the Poisson-Boltzmann equation, yielding ΔC_p^{water}. The coupling term was then obtained using

$$\Delta C_p^{coupling} = \Delta C_p^{el} - \Delta C_p^{ions} - \Delta C_p^{water} \quad (8)$$

Atomic charge parameters

Most charge parameter sets currently used for FDPB calculations have been optimized for reproducing physical quantities (e.g., the free energy of hydration) which do not necessarily have the same parameter dependence as the heat capacity. Thus, before calculating ΔC_p^{el} for macromolecular binding reactions, several parameter sets were compared in order to establish which most accurately reproduced the heat capacity changes associated with the hydration of small ions. In particular, we focused on those ions which represent the charged functional groups found on proteins and nucleic acids. Models of NH_4^+, HCO_2^-, and $H_2PO_4^-$ were built and minimized using *InsightII* and *Discover 2.9* (Molecular Simulations Inc., San Diego, CA), respectively. ΔG^{hyd} for each ion was determined by calculating the difference in the electrostatic energy of the ion in vacuum and solution. ΔC_p^{hyd} was determined by van't Hoff analysis as described above. In addition to formal charges, the PARSE (Sitkoff et al., 1994), CVFF (Hagler et al., 1974), and AMBER (Weiner et al., 1986) partial charge parameters were compared in this analysis.

Molecular structures and heat capacity measurements

All binding reactions were treated as rigid-body associations (i.e., with no binding-associated conformational changes). Crystal structure coordinates

for the complexes were obtained from the Brookhaven protein database. The reactions investigated included the minor groove binding drugs DAPI (1D30) (Rentzeperis et al., 1995), lexitropsin (1LEX, 1LEY) (Goodsell et al., 1995), netropsin (101D, 121D) (Kopka et al., 1985; Tabernero et al., 1993), and Hoechst 33258 (296D) (Vega et al., 1994), and the protein ligand λ repressor DNA binding domain (1LMB) (Beamer and Pabo, 1992). Calculations on the netropsin complex were repeated with two different DNA targets. A second analysis was also performed for the lexitropsin:DNA complex because the orientation of the drug on the DNA is uncertain. Calculations were therefore performed on structures of both possible orientations (1LEX, 1LEY). Heat capacity measurements were taken from Merabet and Ackers (1995) for λ repressor complex, from Haq et al. (1997) for Hoechst 33258, and from Rentzeperis et al. (1995) for netropsin.

Area-based model

Solvent accessible surface areas were calculated with the program SUR-FCV (Sridharan et al., 1992) using a solvent probe radius of 1.4 Å. The heat capacity change associated with binding was computed from the area-based model according to Spolar et al. (1992):

$$\Delta C_p^{surface\ area} = (0.32 \pm 0.04)\Delta A_{nonpolar} \quad (9)$$
$$- (0.14 \pm 0.04)\Delta A_{polar}$$

Calculations were also performed using the area coefficients determined by Freire et al. [0.45 and 0.265 for the nonpolar and polar surfaces, respectively, (Murphy and Freire, 1992)]. Phosphorus, nitrogen, and oxygen atoms were considered polar; all other atoms were considered nonpolar.

Analytical test cases

For the case of a spherical ion or molecule in a salt solution an analytical solution for the linear Poisson-Boltzmann equation is available (Tanford, 1961). The Born model of ion solvation gives the heat capacity associated with the transfer of a spherical ion from vacuum to pure water as

$$\Delta C_p = \frac{q^2}{2a}\left[\frac{2}{\varepsilon^3}\left(\frac{d\varepsilon}{dT}\right)^2 - \frac{1}{\varepsilon^2}\frac{d^2\varepsilon}{dT^2}\right] \quad (10)$$

The Debye-Hückel theory provides an expression for determining the contribution of salt to the solvation free energy of a spherical ion, ΔG^{dh}:

$$\Delta G^{dh} = \frac{-q^2}{2\varepsilon}\frac{\kappa}{(1 + \kappa \cdot a)} \quad (11)$$

where q is the charge, a is the radius of the ion, $\kappa^2 = 8\pi e^2 I/1000\varepsilon kT$ is the Debye-Hückel parameter, and I is the ionic strength. Using the experimental temperature dependence of the water dielectric, the heat capacity contributions for an ion of +1 charge and a radius of 2.50 Å were obtained analytically from Eq. 10, and numerically from the temperature dependence of Eq. 11 using Eq. 5. These were compared to solutions obtained using the FDPB method. For the nonlinear Poisson-Boltzmann equation, no analytical solution for the spherical ion is available. However, solutions can be obtained using the one-dimensional (1-D) finite difference method in reciprocal space using spherical coordinates, as described previously (Sharp and Honig, 1990). This method provides essentially exact solutions with no boundary representation errors for the spherical test case.

Estimation of the precision of the calculations

The precision of our calculations of ΔC_p was estimated as follows. The error in ΔG_{bind}^{el} at each temperature was estimated by the standard deviation of this value for 12 different mappings onto the finite difference grid. These standard deviations were then used to weight the points in the SVD fit to

TABLE 1 Test of heat capacity changes for a spherical ion

	Heat Capacity Change* (cal/mol/K)	
Model	Born Model	Debye Hückel Model
Linear FDPB	-6.25 ± 0.2 ($-5.5^{\#}$)	1.63 ± 0.06 ($1.8^{\S}$)
Nonlinear FDPB	n/a	1.96 ± 0.02 ($2.0^{\P}$)

*For an ion of charge 1, radius 2.5 Å in 0.125 M 1-1 salt at 305 K. Analytical results are in parentheses.
[#]Using Eq. 10.
[§]Using Eq. 11.
[¶]Using 1-D finite difference solutions.

Eq. 5. The standard error in the fitted heat capacity was then obtained using the mean squared error in the fit and the covariance matrix provided by the SVD routine (Johnson and Faunt, 1992; Press et al., 1986).

RESULTS

Table 1 compares the heat capacity obtained from an analytical solution for spherical ion hydration in pure water, in a 0.125 M salt solution using the linear PB equation, and using the nonlinear PB equation. The FDPB and analytical results agree to within 10%. In addition, the table shows a comparison of the linear PB equation and the nonlinear PB equation. The nonlinear case produces a somewhat larger decrease in heat capacity. The difference between analytical and numerical results is within the precision of the finite difference calculations (determined by the standard deviation in heat capacities calculated at multiple positions of the grid), which is quite high (Table 1).

The heat capacity change associated with the hydration (ΔC_p^{hyd}) of NH_4^+, HCO_2^-, and $H_2PO_4^-$ will be dominated by electrostatics and can be directly compared to experiment, as shown in Table 2. Using the partial charge distributions from the CVFF parameter set models (Dauber-Osguthorpe et al., 1988), fairly good agreement was obtained for ΔC_p^{hyd} for NH_4^+ and HCO_2^-, while the most accurate representation of $H_2PO_4^-$ was achieved by assigning a formal charge of -1 to the phosphate atom. For the nucleic acid, a charge of -1 was assigned to each phosphorus atom. Formal charges were assigned to the charged groups on the drugs according to Table 3. Improved agreement can be obtained only at the expense of using unrealistic radii and/or charge distributions indicating that one is reaching the limit of a continuum solvent model, so further parametrization was not pursued.

The van't Hoff plot of electrostatic binding free energy versus temperature for DAPI:DNA binding is shown in Fig. 1. The three curves represent the binding free energy as a

TABLE 2 Heat capacities of hydration for small ions

	Hydration Heat Capacity	
Ion	Experiment*	Calculated
NH_4^-	-6.9	-8.6 ± 0.2
HCO_2^-	-11.0	-10.3 ± 0.2
$H_2PO_4^-$	-4.5	-8.6 ± 0.2

*Marcus, 1994.

TABLE 3 Atomic charge parameters

Drug	Charged Atoms	Assigned Charge	Total Charge on Drug
DAPI	N2, N3, N4, N5	$+0.5$	$+2.0$
Lexitropsin	N1, N2, N9, N10	$+0.5$	$+2.0$
Netropsin	N1, N2, N9, N10	$+0.5$	$+2.0$
Hoechst 33268	N6	$+1.0$	$+1.0$

function of temperature where 1) both Boltzmann and dielectric factors vary, 2) the Boltzmann factor is held constant, and 3) the dielectric is held constant. The curves cross at the chosen reference temperature ($T_0 = 293$ K), since the Boltzmann and dielectric factors are identical at this point. Based on the small curvature of the plots it can be inferred that, in general, the heat capacity change due to electrostatics is small. These basic features of the van't Hoff plot were similar for all cases of DNA ligand binding studied.

Experimental binding heat capacity data, where available, are shown in Table 4, along with results from the FDPB method and the surface area model using the calculated surface areas listed in Table 5. The surface area model does not agree well with experimental values for any of these reactions, making it impossible to reliably interpret the contributions of nonpolar and polar dehydration to binding.

For the FDPB calculations, the fitted values for ΔC_p^{el} show that overall, electrostatic interactions contribute a positive heat capacity change. The total ΔC_p^{el} is dominated by a positive term arising from the water dipole rearrangement which is opposed by the contribution of mobile solvent ions. The ion contribution is negative, and smaller in magnitude than the water dipole term, constituting ~ 30–40% of the total change for the drugs, and only $\sim 3\%$ of the total for the protein. ΔC_p^{el} is not simply the sum of ΔC_p^{ions}
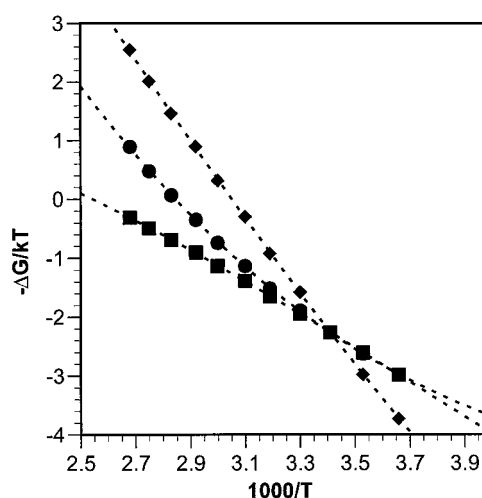

FIGURE 1 van't Hoff plot of DAPI:DNA binding in 0.10 M salt. The symbols represent data points calculated according to the procedure described in the text; the dotted lines are the results of a linear fit to the integrated van't Hoff equation. (◆) ΔC_p^{el}, varying both Boltzmann and dielectric factors; (■) ΔC_p^{ions}, Boltzmann factor kept constant; (●) ΔC_p^{water}, dielectric held constant.

TABLE 4　Heat capacity changes for ligand-DNA binding

		Area Model*		FDPB Model			
Ligand	Expt	Spolar et al.	Freire et al.	Total	Ions	Dipoles	Coupling
DAPI	na	−77	−91	30 ± 0.5	−10 ± 0.2	63 ± 1	−23
Lexitropsin (LEX)	na	−153	−190	39 ± 1	−15 ± 0.7	82 ± 1	−28
Lexitropsin (LEY)	na	−153	−191	35 ± 1	−16 ± 0.7	80 ± 2	−28
Netropsin (101D)	∼0[#]	−172	−218	35 ± 0.3	−13 ± 1	72 ± 1	−24
Netropsin (121D)	∼0[#]	−178	−226	34 ± 0.7	−15 ± 2	70 ± 1	−21
Hoechst 33258	−330[§]	−236	−319	15 ± 14	−7 ± 3	8 ± 14	13
λ repressor bd	−550[¶]	−202	−149	92 ± 1	−3 ± 2	223 ± 4	−129

The heat capacity change from experimental data where available, or calculated from the surface area or the FDPB models. Values are expressed in cal/mol/K.

*Murphy and Freire, 1992; Spolar et al., 1992.

[#]Rentzeperis et al., 1995.

[§]Haq et al., 1997.

[¶]Merabet and Ackers, 1995.

and ΔC_p^{water}, however. A cross-term, $\Delta C_p^{coupling}$, which describes the coupling of dipolar and ionic terms, also makes a substantial contribution to the overall heat capacity change. With the exception of the Hoechst 33258 ligand, the coupling term is negative. Thus, neglecting this cross-term generally results in a 60% increase in the total ΔC_p^{el}.

The surface area model includes a contribution from polar surface area, and thus includes short-range electrostatic interactions. Hence, the surface area and electrostatic terms cannot be directly combined without some double counting of the electrostatic interactions. Nevertheless, information can be extracted from the sign of ΔC_p^{el}. In the case of netropsin, ΔC_p^{el} is of the appropriate sign to close the gap between the experiment and area-based models. Thus, in cases where ΔC_p^{bind} is small, long-ranged electrostatics may play a significant role in the net heat capacity change from solvation upon binding. In instances where the overall heat capacity change is large (as in most binding reactions involving proteins), the magnitude of ΔC_p^{el} is not large enough, and of the wrong sign, to account for the underestimation of the heat capacity change by the area models.

Calculations for the DNA-λ repressor binding domain interaction were performed using both CVFF partial atomic charges and formal charges (charges assigned only to the ionized groups). The calculated heat capacity changes were within 10% of each other (Table 4), indicating that the major contribution comes from the ionized groups, with a

smaller contribution coming from the protein dipolar groups.

The binding of the λ repressor to DNA was studied at salt concentrations ranging from 0.0 to 0.25 M. The calculated heat capacities are shown as a function of ionic strength in Fig. 2. The total ΔC_p^{el} shows a roughly exponential dependence on salt, as does the water dipole term. ΔC_p^{ions}, however, is independent of ionic strength.

DISCUSSION

The goal of this work has been to show that a continuum solvent electrostatics model can be used to study heat capacity effects in DNA-ligand interactions. In applying the FDPB model to the study of heat capacity changes of DNA-ligand binding, there are three problems. The first is to obtain sufficiently accurate numerical solutions to the PB equations. This is a challenge because larger numerical uncertainties are unavoidable for heat capacity calculations

TABLE 5　Solvent accessible surface area changes

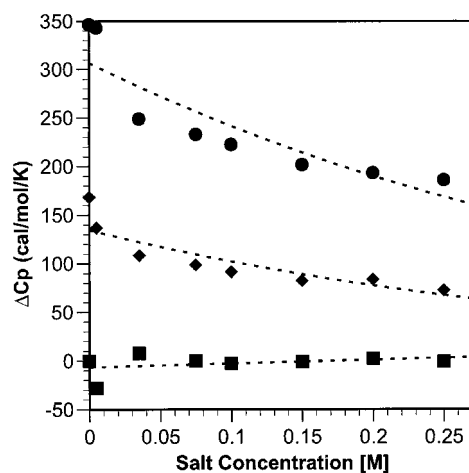|	Area Change (Å[2])		
Ligand	Nonpolar	Polar	Total
DAPI	−356	−261	−618
Lexitropsin (LEX)	−633	−358	−991
Lexitropsin (LEY)	−639	−365	−1004
Netropsin (101D)	−684	−337	−1021
Netropsin (121D)	−715	−361	−1076
Hoechst 33258	−820	−188	−1009
λ repressor bd	−1501	−1987	−3488

FIGURE 2　Salt dependence of ΔC_p^{el} for λ repressor bd:DNA binding. (●) ΔC_p^{el}, varying both Boltzmann and dielectric factors; (■) ΔC_p^{ions}, Boltzmann factor kept constant; (◆) ΔC_p^{water}, dielectric held constant.

(compared with the more common use of FDPB to obtain free energies), since the former requires calculation of the second derivative with respect to temperature. Experimental determinations of heat capacity using the van't Hoff method are not free from this problem either (Chaires, 1996), and this is one of the reasons our understanding of heat capacity changes is poor. Comparison with analytical test cases in Table 1 shows that reasonably accurate solutions can be obtained.

The second problem is to obtain realistic parameters for use in the model. For the FDPB model, the key parameters are the atomic charges and radii. Suitable data for parametrizing heat capacity changes are sparse. Anticipating the dominant role of the formally charged groups, we used experimental data from small ions representing the major ionizable groups of the molecules we were studying. Fair agreement could be obtained, but extensive parametrization to obtain exact agreement with experimental values is not warranted in light of the limitations of the continuum model. This leads to the third problem in using the FDPB model for heat capacities. Representation of the solvent through a dielectric continuum plus a Boltzmann distribution of ions is inherently limited. The use of the known temperature dependence of the dielectric constant provides a good way to incorporate the complex behavior of water in a computationally tractable way. However, specific structural changes in water are known to be important in heat capacity changes (Madan and Sharp, 1997; Sharp and Madan, 1997), so there is a limit to how far one can meaningfully parametrize the FDPB model. Nevertheless, since the electrostatic contribution to the heat capacity change is dominated by the dielectric behavior of water, this method is likely to capture the direction and magnitude of such effects. Direct determination of heat capacity effects using atomic level simulations with current technology has been shown to be impractical even for small solutes (Madan and Sharp, 1996), let alone macromolecules. At this time, then, the FDPB method is also the only way we are aware of for estimating the electrostatic contributions to the heat capacity change of DNA-ligand binding, especially the salt contributions. Thus, any information that can be obtained about the sign and magnitude of these effects will increase our understanding of heat capacity changes.

In part this work was motivated by the observation that the Born model for spherical ion hydration qualitatively reproduces the observed negative heat capacity changes for small ions. Since the enthalpy and entropy of hydration of these ions are also negative, this result is quite puzzling, because it means that the entropy decrease induced in the water by the ion increases with increasing temperature, and that the enthalpic interaction with the water also becomes more favorable (increasingly negative) with increasing temperature. The qualitative success of the Born model in reproducing this effect relies on the inclusion of the experimental temperature dependence of the dielectric constant. This does not, however, provide a molecular interpretation. Even with an analytical expression for the heat capacity in

this model (Eq. 10), the sign of ΔC_p is not immediately apparent, depending as it does on the difference in two temperature derivatives of the dielectric constant of water. However, previous work on simulating heat capacity changes around polar and nonpolar solutes (Sharp and Madan, 1997) suggests the following explanation: water is a highly structured liquid, and this structuring limits the ability of nearby waters to align their dipoles with the field from the ion. As the temperature is increased, the water structure is broken down, allowing the dipoles to more fully align with the ion field, resulting in a greater decrease in net entropy, and a stronger enthalpic interaction. This explains the observed negative heat capacity for the Born model seen in Tables 1 and 2. Since the known temperature dependence of the dielectric constant reflects these subtle structural effects, they will appear in the Born model.

The interaction of the ion with other solvent ions, as with the water dipoles, has a favorable enthalpy and an unfavorable entropy, yielding a net favorable free energy. However, the heat capacity contribution is positive (Table 1). This more "expected" behavior can be simply understood as being caused by increased thermal motion disordering the ion's double layer, resulting in a smaller decrease in entropy induced at higher temperature by the ion (i.e., a positive ΔC_p).

From the spherical ion results, we can understand the observed sign of the heat capacity changes for DNA-ligand binding shown in Table 4. The general direction of the water dipole and ion atmosphere contributions to the solvation heat capacity of polar molecules like DNA, protein, and drugs is expected to follow that of the spherical ions (i.e., to be negative and positive, respectively). In a binding reaction, each molecule is desolvated by its partner and thus interacts less strongly with the water dipoles and ion atmosphere. This will result in heat capacity changes of the opposite sign from electrostatic interactions with the water dipoles and the ion atmosphere (positive and negative, respectively), as observed. The magnitude of the interaction of the DNA and ligand molecules is greatest with the water dipoles, as with the spherical ion, so that the net heat capacity change from electrostatic interactions for binding is positive. In the Poisson-Boltzmann model the alignment of a water dipole depends on the mean electrostatic field, which in turn depends on the mean ion distribution. The reverse is also true. Thus, the dipolar and ionic contributions are coupled, although the sign of this coupling term cannot be anticipated a priori. In most cases this coupling is negative, opposing the dipolar term, but in one case (Hoechst 33258) it is positive. For the protein ligand, the calculations show that ionizable groups produce a larger heat capacity contribution than the protein dipolar groups. This is attributable to the longer-ranged monopolar fields from the former.

Our major conclusion from this work is that electrostatic contributions to heat capacity changes upon binding are significant, but that overall the magnitude of ΔC_p^{el} is not

very large. Therefore, electrostatics would only make a significant contribution to the net heat capacity change in instances where ΔC_p^{bind} itself is small. The sign of ΔC_p^{el} is positive, in accordance with experimental heat capacity data for the burial of polar groups. Since the amount of nonpolar surface buried in binding is usually comparable to or greater than the polar surface area, and since surface area models attribute a larger effect per unit surface area to the nonpolar groups, these models almost always predict a substantial decrease in heat capacity upon binding, and are thus unable to provide an explanation for binding reactions with essentially no heat capacity change. Electrostatic interactions provide a possible explanation for this. However, we conclude from this work that electrostatic interactions can be ruled out as a contributor to the "anomalously" large decrease in heat capacity seen in some protein-DNA binding reactions. Finally, we find that while both the total electrostatic heat capacity change and ΔC_p^{water} exhibit salt-dependent behavior, ΔC_p^{ions} does not.

REFERENCES

Anderson, C., and M. Record. 1993. Salt dependence of oligoion polyion binding: a thermodynamic description based on preferential interaction coefficients. *J. Phys. Chem.* 97:7116–7126.

Anderson, C. F., and M. T. Record. 1982. Polyelectrolyte theories and their application to DNA. *Ann. Rev. Phys. Chem.* 33:191.

Beamer, L. J., and C. O. Pabo. 1992. Refined 1.8 angstroms crystal structure of lambda repressor-operator complex. *J. Mol. Biol.* 227:177.

Ben-Naim, A., and Y. Marcus. 1984. Solvation thermodynamics of nonionic solutes. *J. Chem. Phys.* 81:2016–2027.

Bruccoleri, R. E., J. Novotny, K. A. Sharp, and M. E. Davis. 1996. Finite difference Poisson-Boltzmann electrostatic calculations: increased accuracy achieved by harmonic dielectric smoothing and charge anti-aliasing. *J. Comp. Chem.* 18:268–276.

Chaires, J. B. 1996. Possible origin of differences between van't Hoff and calorimetric enthalpy estimates. *Biophys. Chem.* 64:15–23.

Connelly, P. R., J. A. Thomson, M. J. Fitzgibbon, and F. J. Bruzzese. 1993. Probing hydration contributions to the thermodynamics of ligand binding by proteins. Enthalpy and heat capacity changes of tacrolimus and rapamycin binding to FK506 binding protein in D_2O and H_2O. *Biochemistry.* 32:5583–5590.

Dauber-Osguthorpe, P., V. A. Roberts, D. J. Osguthorpe, J. Wolff, M. Genest, and A. T. Hagler. 1988. Structure and energetics of ligand binding to proteins: *E. coli* dihydrofolate reductase-trimethoprim, a drug-receptor system. *Proteins Struct. Func. Genet.* 4:31–47.

Freire, E. 1995. Forces and factors that contribute to the structural stability of membrane proteins. *Biochim. Biophys. Acta.* 1241:295–322.

Gilson, M., and B. Honig. 1986. The dielectric constant of a folded protein. *Biopolymer.* 25:2097–2119.

Gilson, M., K. A. Sharp, and B. Honig. 1988. Calculating the electrostatic potential of molecules in solution: method and error assessment. *J. Comp. Chem.* 9:327–335.

Goodsell, D. S., H. L. Ng, M. L. Kopka, J. W. Lown, and R. E. Dickerson. 1995. Structure of a dicationic monoimidazole lexitropsin bound to DNA. *Biochemistry.* 34:16654.

Hagler, A. T., E. Huler, and S. Lifson. 1974. Energy functions for peptides and proteins. I. Derivation of a consistent force field including the hydrogen bond from amide crystals. *J. Am. Chem. Soc.* 96:5319–5327.

Haq, I., J. E. Ladbury, B. Z. Chowdhry, T. C. Henkins, and J. B. Chaires. 1997. Specific binding of Hoechst 33258 to the d(CGCAATTTGCG)$_2$ duplex: calorimetric and spectroscopic studies. *J. Mol. Biol.* 271: 244–257.

Hecht, J. L., and B. Honig. 1995. Electrostatic potentials near the surface of DNA—comparing theory and experiment. *J. Phys. Chem.* 99: 7782–7786.

Jayaram, B., K. A. Sharp, and B. Honig. 1989. The electrostatic potential of B-DNA. *Biopolymers.* 28:975–993.

Johnson, M., and L. Faunt. 1992. Parameter estimation by least-squares methods. *Methods Enzymol.* 210:1–37.

Kopka, M. L., C. Yoon, D. S. Goodsell, P. Pjura, and R. E. Dickerson. 1985. Binding of an antitumor drug to DNA. Netropsin and CGCGAAT-TBrCGCG. *J. Mol. Biol.* 183:553.

Lide, D. R. 1990. CRC Handbook of Chemistry and Physics. CRC Press, Boca Raton, FL.

Madan, B., and K. A. Sharp. 1996. Heat capacity changes accompanying hydrophobic and ionic solvation: a Monte Carlo and random network model study. *J. Phys. Chem.* 100:7713–7721.

Madan, B., and K. A. Sharp. 1997. Molecular origin of hydration heat capacity changes of hydrophobic solutes: perturbation of water structure around alkanes. *J. Phys. Chem. B.* 101:11237–11242.

Makhatadze, G., and P. Privalov. 1990a. I. Partial molar heat capacity of individual amino acid residues in aqueous solution: hydration effect. *J. Mol. Biol.* 213:375–384.

Makhatadze, G., and P. Privalov. 1990b. II. Partial molar heat capacity of individual amino acid residues in aqueous solution: protein unfolding effects. *J. Mol. Biol.* 213:385–391.

Marcus, Y. 1994. A simple empirical model describing the thermodynamics of hydration of ions of widely varying size. *Biophys. Chem.* 51: 111–128.

Merabet, E., and G. K. Ackers. 1995. Calorimetric analysis of lambda cI repressor binding to DNA operator sites. *Biochemistry.* 34:8554–8563.

Misra, V., J. Hecht, K. Sharp, R. Friedman, and B. Honig. 1994a. Salt effects on protein-DNA interactions: the lambda cI repressor and ecoR1 endonuclease. *J. Mol. Biol.* 238:264–280.

Misra, V., K. Sharp, R. Friedman, and B. Honig. 1994b. Salt effects on ligand-DNA binding: minor groove antibiotics. *J. Mol. Biol.* 238: 245–263.

Murphy, K., and E. Freire. 1992. Thermodynamics of structural stability and cooperative folding behavior in proteins. *Adv. Protein Chem.* 43: 313–361.

Murphy, K., and S. Gill. 1990. Group additivity thermodynamics for the dissolution of solid cyclic dipeptides into water. *Thermochim. Acta.* 172:11–20.

Nicholls, A., and B. Honig. 1991. A rapid finite difference algorithm utilizing successive over-relaxation to solve the Poisson-Boltzmann equation. *J. Comp. Chem.* 12:435–445.

Press, W., B. Flannery, S. Teukolsky, and W. Vetterling. 1986. Numerical Recipes. Cambridge University Press, Cambridge.

Privalov, P. L., and S. J. Gill. 1988. Stability of protein structure and hydrophobic interaction. *Adv. Protein Chem.* 39:191–234.

Privalov, P., and G. Makhatadze. 1993a. Contribution of hydration to protein folding thermodynamics. I. The enthalpy of hydration. *J. Mol. Biol.* 232:639–659.

Privalov, P., and G. Makhatadze. 1993b. Contribution of hydration to protein folding thermodynamics. II. The entropy and Gibbs free energy of hydration. *J. Mol. Biol.* 232:660–679.

Record, T., M. Olmsted, and C. Anderson. 1990. Theoretical studies of the thermodynamics of ion interaction with DNA. Theoretical Biochemistry and Molecular Biophysics. Adenine Press, New York.

Rentzeperis, D., L. A. Marky, T. J. Dwyer, B. H. Geierstanger, J. G. Pelton, and D. E. Wemmer. 1995. Interaction of minor-groove ligands to an AAATT/AATTT site: correlation of thermodynamic characterization and solution structure. *Biochemistry.* 34:2937–2945.

Robertson, A. D., and K. P. Murphy. 1997. Protein structure and the energetics of protein stability. *Chemical Reviews.* 97:1251–1267.

Sharp, K. A. 1995. Polyelectrolyte electrostatics: salt dependence, entropic

and enthalpic contributions to free energy in the nonlinear Poisson-Boltzmann model. *Biopolymers.* 36:227–243.

Sharp, K. A., R. Friedman, V. Misra, J. Hecht, and B. Honig. 1995. Salt effects on polyelectrolyte-ligand binding: comparison of Poisson-Boltzmann and limiting law counterion binding models. *Biopolymers.* 36:245–262.

Sharp, K., and B. Honig. 1990. Calculating total electrostatic energies with the non-linear Poisson-Boltzmann equation. *J. Phys. Chem.* 94:7684–7692.

Sharp, K. A., and B. Madan. 1997. The hydrophobic effect, water structure and heat capacity changes. *J. Phys. Chem.* 101:4343–4348.

Sharp, K. A., A. Nicholls, and B. Honig. (1990). DelPhi: A Macromolecular Electrostatics Software Package. Copyright Dept. of Biochemistry and Molecular Biophysics. Columbia University, New York.

Sitkoff, D., K. Sharp, and B. Honig. 1994. Accurate calculation of hydration free energies using macroscopic solvent models. *J. Phys. Chem.* 98:1978–1988.

Spolar, R., J. Livingstone, and M. T. Record. 1992. Use of liquid hydrocarbon and amide transfer data to estimate contributions to protein folding. *Biochemistry.* 31:3947–3955.

Spolar, R. S., and M. T. Record. 1994. Coupling of local folding to site-specific binding of proteins to DNA. *Science.* 263:777–784.

Sridharan, S., A. Nicholls, and B. Honig. 1992. A new vertex algorithm to calculate solvent accessible surface areas. *Biophys. J.* 61:995a. (Abstr.).

Sturtevant, J. 1977. Heat capacity and entropy changes in processes involving proteins. *Proc. Natl. Acad. Sci. USA.* 74:2236–2240.

Tabernero, L., N. Verdaguer, M. Coll, I. Fita, G. A. VanDerMarel, J. H. VanBoom, A. Rich, and J. Aymami. 1993. Molecular structure of the A-tract DNA dodecamer d(CGCAAATTTGCG) complexed with the minor groove binding netropsin. *Biochemistry.* 32:8403.

Tanford, C. 1961. Physical Chemistry of Macromolecules. John Wiley and Sons, New York.

Vega, M. C., I. Garcia-Saez, J. Aymami, R. Eritja, G. A. VanDerMarel, J. H. VanBoom, A. Rich, and M. Coll. 1994. Three-dimensional crystal structure of the A-tract DNA dodecamer d(CGCAAATTTGCG) complexed with the minor-groove-binding drug Hoechst 33258. *Eur. J. Biochem.* 222:721.

Weiner, S. J., P. A. Kollman, D. T. Nguyen, and D. A. Case. 1986. An all atom force field for simulations of proteins and nucleic acids. *J. Comp. Chem.* 7:230–252.

Zacharias, M., B. Luty, M. Davis, and J. McCammon. 1992. Poisson-Boltzmann analysis of the lambda repressor-operator interaction. *Biophys. J.* 63:1280–1285.

Zacharias, M., B. Luty, M. Davis, and J. McCammon. 1994. Combined conformational search and finite-difference Poisson-Boltzmann approach for flexible docking. Application to an operator mutation in the lambda repressor-operator complex. *J. Mol. Biol.* 238:455–465.